Reversal of the deleterious effects of chronic dietary HFCS-55 intake by PPAR- agonism correlates with impaired NLRP3 inflammasome activation

Biochem Pharmacol. 2013 Jan 15;85(2):257-64. doi: 10.1016/j.bcp.2012.10.014.
Reversal of the deleterious effects of chronic dietary HFCS-55 intake by PPAR-δ agonism correlates with impaired NLRP3 inflammasome activation.
Collino M, Benetti E, Rogazzo M, Mastrocola R, Yaqoob MM, Aragno M, Thiemermann C, Fantozzi R.
http://www.sciencedirect.com/science/article/pii/S0006295212006909

Reversal of the deleterious effects of chronic dietary HFCS-55 intake by PPAR-δ agonism correlates with impaired NLRP3 inflammasome activation.

Massimo Collino[1§], Elisa Benetti[1δ], Mara Rogazzo[1], Raffaella Mastrocola[2], Muhammed M. Yaqoob[3],Manuela Aragno[2], Christoph Thiemermann[3*] Roberto Fantozzi[1*]

[1] *Department of Drug Science and Technology, University of Turin, Turin, Italy*

[2] *Department of Experimental Medicine and Oncology, University of Turin, Turin, Italy*

[3] *Centre for Translational Medicine and Therapeutics, William Harvey Research Institute, Barts and the London School of Medicine and Dentistry, Queen Mary University of London, London, UK*

[4] *Department of Clinical Pathophysiology, University of Turin, Turin, Italy*

§*Both authors contributed equally to this work.*

**Both authors contributed equally to this work.*

Address all correspondence and requests for reprints to:

Massimo Collino, Department of Drug Science and Technology, University of Turin, via P. Giuria 9, 10125 Torino, Italy. Tel: +39 011 6707955. Fax: +39 011 2367955., e-mail: massimo.collino@unito.it

ABSTRACT

Although high-fructose corn syrup (HFCS-55) is the major sweetener in foods and soft-drinks, its potential role in the pathophysiology of diabetes and obesity ("diabesity") remains unclear. Peroxisome-proliferator activated receptor (PPAR)-δ agonists have never been tested in models of sugar-induced metabolic abnormalities. This study was designed to evaluate (i) the metabolic and renal consequences of HFCS-55 administration (15% wt/vol in drinking water) for 30 weeks on male C57Bl6/J mice and (ii) the effects of the selective PPAR-δ agonist GW0742 (1 mg/kg/day for 16 weeks) in this condition. HFCS-55 caused (i) hyperlipidemia, (ii) insulin resistance, and (iii) renal injury/inflammation. In the liver, HFCS-55 enhanced the expression of fructokinase resulting in hyperuricemia and caused abnormalities in known insulin-driven signaling events. In the kidney, HFCS-55 enhanced the expression of the NLRP3 (nucleotide-binding domain and leucine-rich-repeat-protein 3) inflammasome complex, resulting in caspase-1 activation and interleukin-1β production. All of the above effects of HFCS-55 were attenuated by the specific PPAR-δ agonist GW0742. Thus, we demonstrate for the first time that the specific PPAR-δ agonist GW0742 attenuates the metabolic abnormalities and the renal dysfunction/inflammation caused by chronic HFCS-55 exposure by preventing upregulation of fructokinase (liver) and activation of the NLRP3 inflammasome (kidney).

Keywords: high-fructose corn syrup; PPAR-δ; GW0742; insulin resistance; inflammation

1. Introduction

Type 2 diabetes and obesity, recently referred to as "diabesity," represent two closely linked healthcare challenges of modern societies that continue to rise in prevalence, with devastating health and economic implications [1]. The drastic increase in the incidence of "diabesity" over the past few decades in the Western countries coincided with a substantial increase in the consumption of different dietary components. Along with an increase in total energy consumption, during recent decades, there has been a shift in the types of nutrients that are ingested, including the dramatic increased consumption of fructose, primarily from high-fructose corn syrup (HFCS-55), used as ingredients in processed or prepared foods and caloric beverages [2]. Saccharose contains equimolar quantities of fructose and glucose whereas HFCS-55 syrup, synthesized by refining corn starch, contains 55% fructose and 42% glucose. Because of the higher fructose concentration, the consumption food and soft drinks sweetened with HFCS-55 results in higher fructose than sucrose levels in the systemic circulation. HFCS-55 was developed in 1977 and to date accounts for over 40% of all added caloric sweeteners [3]. Excessive intake of fructose has been linked epidemiologically with increased prevalence of abdominal obesity, insulin resistance, dyslipidemia and, more recently, hyperuricemia and chronic renal disease [4]. The cause-effect relationship between increase in fructose intake and metabolic abnormalities is difficult to prove in human studies. Thus, the animal model described in this article was developed to investigate the metabolic effects of chronic HFCS-55 consumption and to investigate the molecular mechanisms which underlie the observed pathophysiological alterations. Several studies suggest that chronic inflammation is one of the most important key feature of the pathophysiology of diabetes and the metabolic syndrome [5]. Many inflammatory mediators, such as cytokines and cytokine-like proteins known as "adipokines" and "myokines", have been linked to the development of both obesity and insulin resistance [6]. One of the most recently identified protein complexes implicated in obesity-associated insulin resistance and type 2 diabetes is the NLRP3 (nucleotide-binding

domain and leucine-rich repeat protein 3) inflammasome [7, 8]. The NLRP3 inflammasome is a large multimeric danger-sensing platform that promotes autocatalytic activation of the cysteine protease caspase-1 and mediates the cleavage of inactive pro-IL-1β, among other proteins, into its active form [9]. However, the nature of the inflammasome-activating danger signal(s) in diet-induced obesity and insulin resistance are not known.

Peroxisome-Proliferator Activated Receptors (PPARs) are ligand-activated transcription factors belonging to the nuclear receptor superfamily, that exert a critical role in regulating glucose and lipid metabolism. So far, three PPAR isoforms have been identified in mammals: PPAR-α (NR1C1) and PPAR-γ (NR1C3) are the targets for drugs used for the treatment of hypertriglyceridemia and insulin resistance, respectively, whereas the role of the third isoform, PPAR-β/δ (NR1C2, called PPAR-δ below), is less well understood [10]. Recent studies have demonstrated that PPAR-δ activation with specific ligands lowers triglyceride levels and improves the sensitivity to insulin [11]. In addition, specific ligands of PPAR-δ cause potent anti-inflammatory effects in animal models of systemic inflammation [12]. However, the potential beneficial effects of PPAR-δ agonism in metabolic disorders associated with high-added sugar intake and the related molecular mechanisms have never been investigated. Hence, the present study was undertaken to determine whether chronic administration of the selective PPAR-δ agonist GW0742 in mice fed a HFCS-55 diet for 30 weeks may ameliorate sugar-induced diabesity and its renal consequences.

2. Materials and methods

2.1 Animals and diets.

Four-week-old male C57BL6/J mice (Harlan-Italy; Udine, Italy) were housed in a controlled environment at 25±2 °C with alternating 12-h light and dark cycles. They were provided with a Piccioni pellet diet (n.48, Gessate Milanese, Italy) and water *ad libitum*. All the animals were fed with a normal pellet diet for 1 week prior to the experimentation. The animals were then allocated to two dietary regimens, chow diet and normal drinking water (control) or a chow diet and 15% (wt/vol) HFCS-55 solution in drinking water (HFCS) for 30 weeks. All diets contained a standard mineral and vitamin mixture. The concentration of HFCS-55 solution as well as the period of dietary manipulation were chosen according to previous animal studies investigating the metabolic effects of long-term (6–7 months) access to HFCS-55 [13, 14]. Body weight, water, and food intake were recorded weekly. Animal care was in compliance with Italian regulations on the protection of animals used for experimental and other scientific purposes (D.M. 116/92) and the experimental protocol used here has been approved by the Turin University Ethics Committee.

2.2 Drug administration.

After the initial period of 14 weeks of dietary manipulation, each diet group was further subdivided into four different treatment groups: chow diet and normal drinking water (control, *n=10*), chow diet supplemented with GW0742 (1 mg/kg/day) and normal drinking water (control+GW, *n=6*), chow diet and 15% (wt/vol) HFCS-55 solution in drinking water (HFCS, *n=10*), and chow diet supplemented GW0742 (1 mg/kg/day) and 15% (wt/vol) HFCS-55 solution in drinking water (HFCS+GW, *n=10*). The drug was daily administered with the food for the last 16 weeks and the mice were allowed to continue to feed on their respective diets until the end of the study. As shown

in Figure 1, GW0742 is a highly potent and selective PPAR-δ agonist (murine EC_{50}: 28 nM for PPAR-δ; 8,900 nM for PPAR-α and > 10,000 nM for PPAR-γ) [15]. The GW0742 dose was chosen according to a previous study demonstrating that 1 mg/kg GW0742 was effective in reducing inflammation and tissue injury in mice fed a high-fat diet, reaching plasma concentrations adequate to selectively activate PPAR-δ without any cross-reactivity with other PPAR isoforms [16].

2.3 Oral glucose tolerance test (OGTT).

One day before the mice were due to be killed, the OGTT was performed after a fasting period of 6 h by administering glucose (2 g/kg) by oral gavage. Once before administration, and 30, 60, 90, 120 and 150 min afterward, blood was obtained from the saphenous vein, and glucose concentration was measured with a conventional Glucometer (Accu-Check Compact kit, Roche Diagnostics Gmbh, Mannheim, Germany).

2.4 Blood pressure measurements.

Systolic blood pressure was assessed after 30 weeks of dietary manipulation as the mean value of ten consecutive measurements obtained in the morning using a tail-cuff sphygmomanometer (IITC; Life Sciences, Woodland Hills, CA). All animals were preconditioned 1 week before each experiments.

2.5 Blood and urine biochemical analysis.

At weeks 16 after the start of the drug treatment (30 weeks of dietary manipulation), the mice were anesthetized with i.p. injection (30 mg/kg) of Zoletil 100 (Laboratoires Virbac, France), and killed by cardiac exsanguination. Blood samples were collected and plasma was isolated. Glycemia was measured using the Accu-Check Compact kit. The liver and the kidney were isolated, weighed and rapidly freeze-clamped with liquid nitrogen and stored at -80°C. The plasma lipid profile was determined by measuring the content of triglyceride (TG), total cholesterol (TC), high-density-lipoprotein (HDL), and low density-lipoprotein (LDL) by standard enzymatic procedures using reagent kits (Hospitex Diagnostics, Florence, Italy). Plasma uric acid was measured by the uricase method (Uric Acid Assay kit Abnova, USA) Plasma insulin and IL-1β levels were measured using enzyme-linked immunosorbent assay (ELISA) kits (Mouse Insulin ELISA, Sylveniusgaten, Sweden). Excretion of urinary albumin was determined using the albumin-to-creatinine ratio (ACR) in 18 hr urine collections. The concentration of creatinine in urine was determined using a creatinine urinary detection kit (Arbor Assays, USA) and that of albumin using a mouse albumin ELISA kit (Bethyl Laboratories Inc.,USA).

2.6 Tissue extracts.

Liver and kidney extracts were prepared as previously described [17, 18]. Briefly, mice liver and kidney were homogenized at 10% (w/v) in a Potter Elvehjem homogenizer (Wheaton, NJ, USA) using a homogenization buffer containing 20 mM HEPES, pH 7.9, 1 mM $MgCl_2$, 0.5 mM EDTA, 1 mM EGTA, 1 mM dithiothreitol (DTT), 0.5 mM Phenylmethyl Sulphonyl Fluoride (PMSF), 5 μg/ml aprotinin, and 2.5 μg/ml leupeptin. Homogenates were centrifuged at 4000 RPM at 4°C for 5 min. Supernatants were removed and centrifuged at 14000 RPM at 4˚C for 40 minutes. The supernatants thus obtained, containing cytosolic proteins were carefully removed. The amount of

protein contained in cytosolic fractions was determined using a BCA protein assay following the manufacturers' instructions. Samples were stored at -80°C until use.

2.7 Liver lipid contents.

Liver was homogenized in 5% Triton X-100. Homogenates were twice heated to 90°C in a water bath for 3 minutes and cool down. Insoluble materials were removed by centrifugation and hepatic TG, TC, LDL and HDL were detected using reagent kits (Hospitex Diagnostics, Florence, Italy).

2.8 Western blot analysis.

About 60 μg total proteins were loaded for Western blot experiments. Proteins were separated by 8% sodium dodecyl sulphate-polyacrylamide gel electrophoresis (SDS-PAGE) and transferred to a polyvinyldenedifluoride (PVDF) membrane, which was then incubated with a primary antibody (rabbit anti- PPAR-δ,1:500; rabbit anti-total GSK-3β, 1:200; goat anti-pGSK-3β Ser9, 1:200; rabbit anti-total Akt, 1:1000; mouse anti-pAkt Ser473, 1:1000; goat anti-ICAM-1, 1:500; rabbit anti-total IRS-2, 1:200; goat anti-pIRS-1/2 Ser270, 1:200; goat anti-ketohexokinase, 1:200; rabbit anti- IL-1β [against both IL-1β precursor and mature IL-1β], 1:200; and rabbit anti-caspasi-1 p10 [against both caspase-1 p10 precursor and cleaved caspase-1 p10], 1:200). Blots were then incubated with a secondary antibody conjugated with horseradish peroxidase (1:10000) and developed using the ECL detection system. The immunoreactive bands were visualised by autoradiography and the density of the bands was evaluated densitometrically using Gel Pro®Analyzer 4.5, 2000 software (Media Cybernetics, Silver Spring, MD, USA). The membranes were stripped and incubated with β-actin monoclonal antibody (1:1000) and subsequently with an anti-rabbit antibody (1:10000) to assess gel-loading homogeneity.

2.9 Myeloperoxidase (MPO) activity.

Samples were homogenized in a solution containing 0.5% (w/v) hexadecyltrimethyl-ammonium bromide dissolved in 50 mmol/L potassium phosphate buffer (pH 6) and centrifuged for 30 min at 13,000g at 4°C. An aliquot of the supernatant was then allowed to react with a solution of 0.167 mg/ml O-dianisidine dihydrochloride and 0.0005% H_2O_2. The rate of change in absorbance was measured spectrophotometrically at 460 nm. MPO activity was defined as the quantity of enzyme degrading 1 μmol of peroxide per min at 37°C and was expressed in milliunits per gram of wet tissue.

2.10 Materials.

Unless otherwise stated, all compounds were purchased from the Sigma-Aldrich Company Ltd. (St. Louis, Missouri, USA). HFCS-55 was from Nature's Flavors (Orange, CA, USA). The BCA Protein Assay kit and SuperBlock blocking buffer were from Pierce Biotechnology Inc. (Rockford, IL, USA) and PVDF was from the Millipore Corporation (Bedford, MA, USA). Antibodies were from Cell-Signaling Technology (Beverly, MA, USA). The anti-mouse, anti-rabbit and anti-goat horseradish peroxidase-linked antibodies were from Santa Cruz Biotechnology (Santa Cruz, CA, USA) and Luminol ECL were from PerkinElmer (Waltham, MA, USA).

2.11 Statistical analysis.

All values in both the text and figures are expressed as mean ± S.D. for *n* observations. One-way analysis of variance with Dunnett's post-hoc test was performed using the GraphPad Prism version

4.02 for Windows (GraphPad Software, San Diego, CA, USA) and p values below 0.05 were considered as significant.

3. Results

3.1 Characteristics of the experimental groups.

As shown in Table 1, mean arterial blood pressure and heart rate were not modified by either dietary manipulation or by drug treatment. In contrast, the body weight gain of the HFCS-55 group significantly increased (>30%) compared to that of the control group after 7 months of feeding, and daily administration of GW0742 induced a slight, but not significant reduction. Mice fed with the experimental diet had a greater liver and adipose tissue (epididymal fat) weight than control diet-fed animals and GW0742 treatment significantly ($p<0.05$) reduced liver and adipose tissue weight. There was a three-fold increase in the triglyceride content in the liver of HFCS-55 mice in comparison with control mice and hepatic triglyceride accumulation was reduced by GW0742 administration. Similarly, GW0742 significantly blunted the diet-induced increase in hepatic levels of cholesterol and increased the hepatic HDL content (Table 1). Similar results on lipid profiles were also obtained when triglycerides, total cholesterol, LDL and HDL were measured in mice serum (Table 2). When compared to control, chronic exposure to HFCS-55 resulted in 30% and 80% increase in fasting serum glucose and insulin levels, respectively, and these changes were suppressed by GW0742 (Table 2). When compared to control, HFCS-55 mice also showed a significant impairment in glucose (Figure 2). Most notably, GW0742 significantly ($p < 0.01$) improved glucose tolerance in HFCS-55 fed mice.

It should be noted that in normal mice GW0742 had no significant effect on any of the above described metabolic parameters.

3.2 GW0742 restored the impaired insulin signaling pathway in the liver of HFCS-55 treated mice.

The deleterious effects of HFCS-55 consumption on glucose tolerance were associated with alterations in the insulin-signaling pathways in the liver (Figure 3). The HFCS-55 diet did not alter the protein expression of the IRS-2, Akt or GSK-3β compared to the control group. However, HFCS-55 caused a significant increase in Ser^{270} phosphorylation of IRS-2 in parallel with high insulin levels and reduced Ser^{473} phosphorylation of Akt (Figure 3A and 3B). Ser^{9} phosphorylation of GSK-3β, a downstream target of Akt, was also reduced in the presence of HFCS-55 (Figure 3C), suggestive of impaired insulin signaling downstream of IRS-2 possibly due to high TG levels both in liver and plasma. Most notably, GW0742 attenuated all of the above effects of HFCS-55 so that the degree of phosphorylation of IRS-2, Akt and GSK-3β observed in HFCS-55 mice treated with GW0742 was not significantly different from those observed in control.

3.3 Effects of GW0742 on hepatic expression of PPAR-δ and fructokinase and serum uric acid levels.

HFCS-55 significantly induced the hepatic expression of PPAR-δ protein, but oral administration of GW0742 for 16 weeks resulted in a further, marked increase in the expression of the protein of this nuclear receptor (Figure 4A). In contrast, the hepatic expression of fructokinase (ketohexokinase), the enzyme that catalyzes the phosphorylation of fructose to produce fructose-1-phosphate, was almost doubled in the HFCS-55 group in comparison with control animals. Interestingly this effect was not seen in HFCS-55 animals treated with GW0742 which suggest that PPAR-δ agonist attenuates HFCS-55 induced fructokinase upregulation. (Figure 4B). A unique characteristic of fructose metabolism by fructokinase is the ability to raise uric acid levels [19]. Here we confirm that fructokinase activation induced by daily consumption of HFCS-55 is associated with a marked increase in serum uric acid concentrations (when compared with control animals; Figure 4C).

Interestingly, administration of GW0742 significantly attenuated the development of hyperuricemia caused by HFCS-55.

3.4 GW0742 reduces the albuminuria evoked by chronic exposure to HFCS-55.

Compared with mice on control diet, mice on a HFCS-55 diet showed significantly increased ACR ratio, which is an indicator of albuminuria and, hence, glomerular injury or inflammation induced tubular proteinuria [20]. In contrast, GW0742 attenuated the increased in urinary albumin caused by HFCS-55 (Figure 5).

3.5 Pharmacological PPAR-δ activation reduced neutrophil infiltration in the kidney evoked by chronic consumption of HFCS-55.

As hyperuricemia and albuminuria are well known markers of renal injury, we investigated whether the beneficial effects of GW0742 were associated with an attenuation of renal inflammation. MPO activity, a marker of neutrophil infiltration, was significantly elevated in the kidneys of mice chronically exposed to HFCS-55 enriched diet (94.11±13.32 μU/g) in comparison with control animals (38.17±7.10 μU/g) (Figure 6A). In GW0742-treated animals subjected to HFCS-55 diet, the MPO activity was significantly reduced (58.33±8.11 μU/g). When compared to control animals, the HFCS-55 diet resulted a significant increase in the expression of ICAM-1 (intercellular adhesion molecule- 1). A similar increase in ICAM-1 expression was not seen in HFCS-55 mice treated with GW0742 (Figure 6B). Similarly, HFCS-55 diet resulted a significant increase in the expression of iNOS, which has been reported to contribute to the neutrophil accumulation in diabetic kidney, while no significant increase in iNOS expression was observed in HFCS-55 mice treated with GW0742 (Figure 6C).

3.6 PPAR-δ agonism prevented NLRP3 inflammasome activation evoked by chronic consumption of HFCS-55 in the kidney.

To explore one of the potential molecular mechanisms underlying the observed anti-inflammatory effects of the PPAR-δ ligand, we measured the expression of the NLRP3 inflammasome protein complex in the kidney (Figure 7). The NLRP3 inflammasome serves as a platform for the activation of caspase-1, which involves autocatalytic processing of the pro-caspase-1 to generate an active form leading to pro–IL-1β cleavage to produce mature IL-1β. In the kidney, PPAR-δ expression was not significantly affected by dietary manipulation, while NLRP3 expression was markedly increased in HFCS-55 mice (compared to normal controls). The increase in PPAR-δ expression afforded by GW0742 in the kidney was associated with a significant reduction in NLRP3 protein levels. NLRP3 up-regulation in the kidneys of HFCS-55 mice was associated with caspase-1 activation as detected by the appearance of the p20 subunit of caspase-1. The end product of NLRP3 inflammasome activation, the active form of the proinflammatory cytokine IL-1β was found in the kidneys of HFCS-55 mice, but not in the kidneys of control animals. Notably, the post-translational processing of procaspase-1 and proIL-1β into the active form of caspase-1 and mature IL-1β was significantly reduced by in kidneys obtained from HFCS-55 mice treated with GW0742. Moreover, treatment of HFCS-55 mice with GW0742 almost completely prevented the rise in the serum concentrations of IL-1β caused by chronic HFCS-55 exposure (Figure 7B)

4. Discussion

Over the past 10 years several observational studies have found positive associations between the consumption of sugar-sweetened beverages and weight gain and development of type 2 diabetes and chronic kidney disease [21-24]. As HFCS-55 represents more than 40% of all caloric sweeteners added to beverages and food, it is surprising that very few studies have investigated the mechanisms underlying the HFCS-55-induced metabolic abnormalities. To our knowledge this is the first study, which investigates a) the effects of chronic HFCS-55 exposure on metabolic and inflammatory signaling pathways and b) its potential pharmacological modulation. To address these issues we examined the effects of chronic administration of the selective PPAR-δ agonist, GW0742, in animals exposed for 30 weeks to a HFCS-55-enriched diet. HFCS-55 was added to the drinking water at a concentration that covers 10% of the daily calorie intake, which corresponds to the average energy intake in the form of ingested sweeteners in the Western diet. Our data clearly demonstrate that chronic HFCS-55 feeding caused a significant increase in body weight and, more importantly dyslipidemia, hyperinsulinemia and an increase in insulin resistance due to impaired insulin signalling.. For instance, HFCS-55 diet increased the phosphorylation of IRS-2, the main transducer of the insulin signal in the liver [25], as well as reduced phosphorylation of the downstream key insulin signaling kinases, Akt and GSK-3β (an Akt substrate) [26], thus evoking a significant impairment of insulin responsiveness. Most importantly, we report here for the first time that all of the metabolic abnormalities caused by HFCS-55 were attenuated in animals that had been treated with a specific PPAR-δ agonist. The changes induced by PPAR-δ agonism on insulin signaling may be secondary to its ability to improve serum and hepatic lipid profiles, as suggested by recent studies showing that increased liver fat content in type 2 diabetic patients significantly contributes to the development of both hepatic and peripheral insulin resistance [27, 28]. Although some studies have reported beneficial effects of PPAR-δ ligands on lipid and glucose metabolism in

mice consuming high fat diets [29-31], this is the first study that demonstrates that PPAR-δ activation is helpful in counteracting the deleterious effects evoked by chronic consumption of high sugar diet. To elucidate the potential mechanisms underlying the beneficial effects of GW0742 reported here, we first focused on the liver, the primary site for fructose metabolism, by measuring the expression levels of its pharmacological target, PPAR-δ, and fructokinase, the main fructose-metabolizing enzyme. We report here that PPAR-δ is expressed in the liver of both control and HFCS-55 fed mice and, more importantly, that its expression is substantially increased by chronic administration of GW0742. The agonist-induced receptor upregulation is a known physiological cellular response to PPAR activation, which has been previously described in other experimental models [32, 33]. In keeping with other studies [34, 35], we also report that HFCS-55 derived dietary fructose induced its own metabolism, by inducing the expression of liver fructokinase. Interestingly, in the presence of marked PPAR-δ activation, the hepatic protein levels of this enzyme were brought to values similar to those measured in control animals. As excessive fructose metabolism by fructokinase induces the production of a large amount of TG and free fatty acids [36], we speculate that the beneficial effects of GW0742 on lipid profiles are due to its ability to break this vicious circle by repressing the gene for fructokinase either by transcriptional transrepression or by interaction with other transcription factors involved in fructokinase gene transcription. Another unique characteristic of fructose metabolism by fructokinase is its ability to raise uric acid levels [37], as also confirmed in our study. The reduction in fructokinase expression in the presence of PPAR-δ activation may, thus, also account for the reduced hyperuricemia afforded by GW0742. Both experimental and clinical studies have previously demonstrated that an increased serum uric acid level can lead to kidney disease [38, 39]. Here we show a significant increase in albuminuria (measured as increase in the albumin/creatinine ratio) in animals chronically exposed to HFCS-55; an effect which was attenuated by GW0742. The NLRP3 inflammasome is one of the most recently identified protein complexes involved in the development of chronic kidney disease [40]. Rats fed

with fructose for 8 weeks showed a significant increase in renal protein levels of NLRP3 [41] and increased levels of uric acid have been shown to directly activate the NLRP3 inflammasome [42]. Here, we demonstrate that the HFCS-55 diet evoked up-regulation of renal NLRP3 expression, resulting in activation of caspase-1 and the subsequent cleavage of pro-IL1β to (the biologically active secreted form) IL-1β. In mice with high fructose diet, the specific PPAR-δ ligand GW0742 reduced NLRP3 expression and activity, resulting in reduced local and systemic levels of IL-1β. The release of cytokines, including IL-1β, from damaged cells or tissues is known to contribute to inflammatory processes by promoting neutrophil chemotaxis and activation [43]. Our results show that chronic HFCS-55 exposure evoked a marked increases in the kidney of (i) MPO activity (a well established marker of neutrophil infiltration), (ii) iNOS and (iii) ICAM-1, the endothelial ligand for the neutrophil receptor CD11b/CD18. There is good evidence that the enhanced expression of iNOS contributes to renal injury and neutrophil accumulation in the diabetic kidney [44]. In addition, the exposure of the vascular endothelium to elevated glucose concentrations induces ICAM-1 expression, while the inhibition of this process ameliorates diabetic nephropathy [45, 46]. In our study, PPAR-δ activation by GW0742 resulted in a significant inhibition of neutrophil infiltration in the mouse kidney. We and others have previously documented similar beneficial effects of PPAR-δ agonists on leukocyte infiltration in different animal models of renal injury [18, 47]. Considering that clinical trials have shown that pharmacological blockade of IL-1β leads to a significant improvement of glycemia and beta-cell secretory function in type 2 patients [48-50], it is likely that the effects of chronic PPAR-δ agonism on insulin sensitivity and kidney injury in our experimental model are due, at least in part, to inhibition of the NLRP3 inflammasome in the kidney. To our knowledge, this is the first paper that demonstrates a correlation between PPAR-δ activation and inhibition of NLRP3 inflammasome activation, thus adding an original piece of evidence to the complex mechanisms by which PPAR-δ can regulate several biological functions. Although a recently published paper has revealed PPAR-γ binding sites in the promoter regions of a member of

the NLRP family of protein [51], to date, the consensus sequence of the PPAR-δ binding site has not yet been identified in the promoter region of the genes encoding elements of the NLRP3 inflammasome complex.

In summary, the chronic exposure to the most widely used added sugar HFCS-55 evokes metabolic abnormalities and renal dysfunction/inflammation, which are attenuated by activation of PPAR-δ. Our results clearly show that the observed beneficial effect of the PPAR-δ ligand GW0742 are associated with prevention of (i) the upregulation of fructokinase (liver) and (ii) activation of the NLRP3 inflammasome (kidney).

Author contributions

E.B., M.R. and R.M. researched data. M.C conceived and performed the study and wrote the manuscript. C.T. and R.F. participated in the interpretation of data and reviewed/edited the manuscript. M.A. and MMY contributed to discussion and revised the manuscript critically for intellectual content. All authors approved the final version of the manuscript.

Conflicts of interest

None to declare.

REFERENCES

[1] Tschop MH, Dimarchi RD. Outstanding scientific achievement award lecture 2011: defeating diabesity: the case for personalized combinatorial therapies. Diabetes 2012;61:1309-14.

[2] Collino M. High dietary fructose intake: Sweet or bitter life? World J Diabetes 2011;2:77-81.

[3] Moeller SM, Fryhofer SA, Osbahr AJ, 3rd, Robinowitz CB. The effects of high fructose syrup. J Am Coll Nutr 2009;28:619-26.

[4] Tappy L, Le KA. Metabolic effects of fructose and the worldwide increase in obesity. Physiol Rev 2010;90:23-46.

[5] Hotamisligil GS. Inflammation and metabolic disorders. Nature 2006;444:860-7.

[6] Feve B, Bastard JP. The role of interleukins in insulin resistance and type 2 diabetes mellitus. Nat Rev Endocrinol 2009;5:305-11.

[7] Stienstra R, van Diepen JA, Tack CJ, Zaki MH, van de Veerdonk FL, Perera D, et al. Inflammasome is a central player in the induction of obesity and insulin resistance. Proc Natl Acad Sci U S A 2011;108:15324-9.

[8] Vandanmagsar B, Youm YH, Ravussin A, Galgani JE, Stadler K, Mynatt RL, et al. The NLRP3 inflammasome instigates obesity-induced inflammation and insulin resistance. Nat Med 2011;17:179-88.

[9] Schroder K, Zhou R, Tschopp J. The NLRP3 inflammasome: a sensor for metabolic danger? Science 2010;327:296-300.

[10] Staels B, Fruchart JC. Therapeutic roles of peroxisome proliferator-activated receptor agonists. Diabetes 2005;54:2460-70.

[11] Benetti E, Patel NS, Collino M. The role of PPARbeta/delta in the management of metabolic syndrome and its associated cardiovascular complications. Endocr Metab Immune Disord Drug Targets 2011;11:273-84.

[12] Kapoor A, Shintani Y, Collino M, Osuchowski MF, Busch D, Patel NS, et al. Protective role of peroxisome proliferator-activated receptor-beta/delta in septic shock. Am J Respir Crit Care Med 2010;182:1506-15.

[13] Bocarsly ME, Powell ES, Avena NM, Hoebel BG. High-fructose corn syrup causes characteristics of obesity in rats: increased body weight, body fat and triglyceride levels. Pharmacol Biochem Behav 97:101-6.

[14] Collison KS, Maqbool ZM, Inglis AL, Makhoul NJ, Saleh SM, Bakheet RH, et al. Effect of dietary monosodium glutamate on HFCS-induced hepatic steatosis: expression profiles in the liver and visceral fat. Obesity (Silver Spring) 18:1122-34.

[15] Sznaidman ML, Haffner CD, Maloney PR, Fivush A, Chao E, Goreham D, et al. Novel selective small molecule agonists for peroxisome proliferator-activated receptor delta (PPARdelta)--synthesis and biological activity. Bioorg Med Chem Lett 2003;13:1517-21.

[16] Takata Y, Liu J, Yin F, Collins AR, Lyon CJ, Lee CH, et al. PPARdelta-mediated antiinflammatory mechanisms inhibit angiotensin II-accelerated atherosclerosis. Proc Natl Acad Sci U S A 2008;105:4277-82.

[17] Collino M, Aragno M, Castiglia S, Miglio G, Tomasinelli C, Boccuzzi G, et al. Pioglitazone improves lipid and insulin levels in overweight rats on a high cholesterol and fructose diet by decreasing hepatic inflammation. Br J Pharmacol 2010;160:1892-902.

[18] Collino M, Benetti E, Miglio G, Castiglia S, Rosa AC, Aragno M, et al. Peroxisome proliferator-activated receptor beta/delta agonism protects the kidney against ischemia/reperfusion injury in diabetic rats. Free Radic Biol Med 2011;50:345-53.

[19] Johnson RJ, Sautin YY, Oliver WJ, Roncal C, Mu W, Gabriela Sanchez-Lozada L, et al. Lessons from comparative physiology: could uric acid represent a physiologic alarm signal gone awry in western society? J Comp Physiol B 2009;179:67-76.

[20] D'Amico G, Bazzi C. Pathophysiology of proteinuria. Kidney Int 2003;63:809-25.

[21] Malik VS, Popkin BM, Bray GA, Despres JP, Willett WC, Hu FB. Sugar-sweetened beverages and risk of metabolic syndrome and type 2 diabetes: a meta-analysis. Diabetes Care 2010;33:2477-83.
[22] Welsh JA, Sharma A, Abramson JL, Vaccarino V, Gillespie C, Vos MB. Caloric sweetener consumption and dyslipidemia among US adults. JAMA 2010;303:1490-7.
[23] Curhan GC, Forman JP. Sugar-sweetened beverages and chronic disease. Kidney Int 2010;77:569-70.
[24] Shoham DA, Durazo-Arvizu R, Kramer H, Luke A, Vupputuri S, Kshirsagar A, et al. Sugary soda consumption and albuminuria: results from the National Health and Nutrition Examination Survey, 1999-2004. PLoS One 2008;3:e3431.
[25] Kim SK, Novak RF. The role of intracellular signaling in insulin-mediated regulation of drug metabolizing enzyme gene and protein expression. Pharmacol Ther 2007;113:88-120.
[26] Cohen P, Goedert M. GSK3 inhibitors: development and therapeutic potential. Nat Rev Drug Discov 2004;3:479-87.
[27] Tatarczyk T, Ciardi C, Niederwanger A, Kranebitter M, Patsch JR, Pedrini MT. Postprandial triglyceride-rich lipoproteins induce hepatic insulin resistance in HepG2 cells independently of their receptor-mediated cellular uptake. Mol Cell Endocrinol 2011;343:71-8.
[28] Kotronen A, Juurinen L, Tiikkainen M, Vehkavaara S, Yki-Jarvinen H. Increased liver fat, impaired insulin clearance, and hepatic and adipose tissue insulin resistance in type 2 diabetes. Gastroenterology 2008;135:122-30.
[29] Barroso E, Rodriguez-Calvo R, Serrano-Marco L, Astudillo AM, Balsinde J, Palomer X, et al. The PPARbeta/delta activator GW501516 prevents the down-regulation of AMPK caused by a high-fat diet in liver and amplifies the PGC-1alpha-Lipin 1-PPARalpha pathway leading to increased fatty acid oxidation. Endocrinology 2011;152:1848-59.
[30] Ye JM, Tid-Ang J, Turner N, Zeng XY, Li HY, Cooney GJ, et al. PPARdelta agonists have opposing effects on insulin resistance in high fat-fed rats and mice due to different metabolic responses in muscle. Br J Pharmacol 2011;163:556-66.
[31] Wu HT, Chen CT, Cheng KC, Li YX, Yeh CH, Cheng JT. Pharmacological activation of peroxisome proliferator-activated receptor delta improves insulin resistance and hepatic steatosis in high fat diet-induced diabetic mice. Horm Metab Res 2011;43:631-5.
[32] Fu J, Gaetani S, Oveisi F, Lo Verme J, Serrano A, Rodriguez De Fonseca F, et al. Oleylethanolamide regulates feeding and body weight through activation of the nuclear receptor PPAR-alpha. Nature 2003;425:90-3.
[33] Miglio G, Rosa AC, Rattazzi L, Grange C, Collino M, Camussi G, et al. The subtypes of peroxisome proliferator-activated receptors expressed by human podocytes and their role in decreasing podocyte injury. Br J Pharmacol 2011;162:111-25.
[34] Vila L, Rebollo A, Adalsteisson GS, Alegret M, Merlos M, Roglans N, et al. Reduction of liver fructokinase expression and improved hepatic inflammation and metabolism in liquid fructose-fed rats after atorvastatin treatment. Toxicol Appl Pharmacol 2011;251:32-40.
[35] Korieh A, Crouzoulon G. Dietary regulation of fructose metabolism in the intestine and in the liver of the rat. Duration of the effects of a high fructose diet after the return to the standard diet. Arch Int Physiol Biochim Biophys 1991;99:455-60.
[36] Nomura K, Yamanouchi T. The role of fructose-enriched diets in mechanisms of nonalcoholic fatty liver disease. J Nutr Biochem 2012;23:203-8.
[37] Lanaspa MA, Tapia E, Soto V, Sautin Y, Sanchez-Lozada LG. Uric acid and fructose: potential biological mechanisms. Semin Nephrol 2011;31:426-32.
[38] Mazzali M, Hughes J, Kim YG, Jefferson JA, Kang DH, Gordon KL, et al. Elevated uric acid increases blood pressure in the rat by a novel crystal-independent mechanism. Hypertension 2001;38:1101-6.

[39] Sanchez-Lozada LG, Tapia E, Santamaria J, Avila-Casado C, Soto V, Nepomuceno T, et al. Mild hyperuricemia induces vasoconstriction and maintains glomerular hypertension in normal and remnant kidney rats. Kidney Int 2005;67:237-47.
[40] Anders HJ, Muruve DA. The inflammasomes in kidney disease. J Am Soc Nephrol 2011;22:1007-18.
[41] Hu QH, Zhang X, Pan Y, Li YC, Kong LD. Allopurinol, quercetin and rutin ameliorate renal NLRP3 inflammasome activation and lipid accumulation in fructose-fed rats. Biochem Pharmacol 2012;84:113-25.
[42] Jin C, Flavell RA. Molecular mechanism of NLRP3 inflammasome activation. J Clin Immunol 2010;30:628-31.
[43] Graca-Souza AV, Arruda MA, de Freitas MS, Barja-Fidalgo C, Oliveira PL. Neutrophil activation by heme: implications for inflammatory processes. Blood 2002;99:4160-5.
[44] Xiao H, Li Y, Qi J, Wang H, Liu K. Peroxynitrite plays a key role in glomerular lesions in diabetic rats. J Nephrol 2009;22:800-8.
[45] Altannavch TS, Roubalova K, Kucera P, Andel M. Effect of high glucose concentrations on expression of ELAM-1, VCAM-1 and ICAM-1 in HUVEC with and without cytokine activation. Physiol Res 2004;53:77-82.
[46] Park CW, Kim JH, Lee JH, Kim YS, Ahn HJ, Shin YS, et al. High glucose-induced intercellular adhesion molecule-1 (ICAM-1) expression through an osmotic effect in rat mesangial cells is PKC-NF-kappa B-dependent. Diabetologia 2000;43:1544-53.
[47] Letavernier E, Perez J, Joye E, Bellocq A, Fouqueray B, Haymann JP, et al. Peroxisome proliferator-activated receptor beta/delta exerts a strong protection from ischemic acute renal failure. J Am Soc Nephrol 2005;16:2395-402.
[48] Larsen CM, Faulenbach M, Vaag A, Volund A, Ehses JA, Seifert B, et al. Interleukin-1-receptor antagonist in type 2 diabetes mellitus. N Engl J Med 2007;356:1517-26.
[49] Larsen CM, Faulenbach M, Vaag A, Ehses JA, Donath MY, Mandrup-Poulsen T. Sustained effects of interleukin-1 receptor antagonist treatment in type 2 diabetes. Diabetes Care 2009;32:1663-8.
[50] Rissanen A, Howard CP, Botha J, Thuren T. Effect of Anti-IL-1beta Antibody (Canakinumab) on Insulin Secretion Rates in Impaired Glucose Tolerance or Type 2 Diabetes: Results of a Randomized, Placebo-Controlled Trial. Diabetes Obes Metab 2012;9999.
[51] Kempster SL, Belteki G, Forhead AJ, Fowden AL, Catalano RD, Lam BY, et al. Developmental control of the Nlrp6 inflammasome and a substrate, IL-18, in mammalian intestine. Am J Physiol Gastrointest Liver Physiol 2011;300:G253-63.

TABLE 1

Effects of chronic *in vivo* treatment of GW0742 on metabolic parameters at 7 months of dietary manipulation

	Control *(n = 10)*	**Control+GW0742** *(n = 6)*	**HFCS** *(n = 10)*	**HFCS+GW0742** *(n = 10)*
Body weight, *g*	32.25±1.67	31.6±2.75	36.00±1.41*	35.00±2.83*
Body weight gain, *g*	11.88±1.13	10.75±2.06	16.00±1.41*	13.88±2.90
Caloric intake (kcal/die)	1.0±0.07	0.87±0.17	1.59±0.15*	1.52±0.18*
Mean Arterial Blood Pressure (mm Hg)	112±5	111±4	101±7	106±5
Heart Rate (beats/minute)	539±38	574±44	571±44	557±33
Epididymal fat weight, (%BW)	3.66±0.29	3.47±0.22	4.22±0.35*	3.86±0.33§
Kidney weight, (%BW)	1.17±0.11	1.20±0.12	1.13±0.32	0.99±0.12
Liver weight, (%BW)	4.49±0.50	4.67±0.74	5.13±0.36*	4.55±0.19§
Liver triglycerides, *µmol/g*	2.69±0.32	3.04±0.42	7.90±0.33*	4.03±0.53*§
Liver cholesterol, *µmol/g*	474.3±38.9	519.8±39.9	691.8±44.8*	623±53.7*§
Liver HDL, *µmol/g*	318.8±43.1	293.6±45.4	345.8±48.2	429.9±48.9*§
Liver LDL, *µmol/g*	59.1±8.8	76.4±14.2	105.9±16.2*	109.2±13.6*

Data are means±S.D. * p< 0.01 vs Control § p< 0.05 vs HFCS

TABLE 2

Effects of chronic *in vivo* treatment of GW0742 on mouse blood chemistry at 7 months of dietary manipulation

	Control	**Control+GW0742**	**HFCS**	**HFCS+GW0742**
	(n = 10)	*(n = 6)*	*(n = 10)*	*(n = 10)*
Glucose, mg/dL	78.67±13.54	76.50±15.45	103.40±11.98*	81.28±10.83§
Insulin, µg/L	1.27±0.07	1.30±0.19	2.26±0.51*	1.51±0.46§
Total cholesterol, mmol/L	2.20±0.08	2.23±0.12	2.46±0.13*	2.15±0.16§
Triglyceride, mmol/L	1.10±0.12	1.07±0.23	1.37±0.11*	0.93±0.21§
HDL, mmol/L	1.28±0.29	1.47±0.35	0.81±0.26*	1.26±0.37§
LDL, mmol/L	0.78±0.17	0.74±0.13	0.99±0.10*	0.73±0.15§

Data are means±S.D. * $p < 0.01$ vs Control § $p < 0.01$ vs HFCS

FIGURE LEGENDS

Figure 1. GW0742 chemical structure and affinity for mouse PPARs isoforms, according to Sznaidman et al. (2003)

Figure 2. Effects of two dietary regimens either normal (Control) or a diet enriched with 15% HFCS-55 solution (HFCS) on oral glucose tolerance in rats treated with GW0742 (1 mg/kg/day, p.o.) (Control+GW; HFCS+GW). Values are mean ± SD of 6–10 animals per group. ★ $P < 0.05$ versus Control.

Figure 3. Effects of GW0742 on insulin signal transduction in the liver of mice fed on a HFCS-55 enriched diet. Total IRS-2 protein expression and Ser^{270} phosphorylation (Panel A), total Akt protein expression and Ser^{473} phosphorylation (Panel B), and total GSK-3β protein expression and Ser^{9} phosphorylation (Panel C) were analyzed by Western blot on the liver obtained from mice fed on a standard (Control) or HFCS-55 diet (HFCS) for 30 weeks and treated with GW0742 (1 mg/kg/day) added during the last 16 weeks (Control + GW; HFCS + GW). Densitometric analysis of the bands is expressed as relative optical density (O.D.), corrected for the corresponding β-actin contents and normalized using the related Control band. The data are means ± SD of three separate experiments. ★ $p < 0.01$ versus Control.

Figure 4. Effects of dietary manipulation and GW0742 treatment on hepatic PPAR-δ (Panel A) and fructokinase (Panel B) expression and hyperuricemia development (Panel C). Protein expression was measured by Western blot analysis in liver homogenates of mice fed with a standard (Control) or HFCS-55 diet (HFCS) in the absence or presence of GW0742 treatment (Control+GW; HFCS+GW). Densitometric analysis of the bands is expressed as relative optical density (O.D.), corrected for the corresponding β-actin and normalized using the related Control band. Serum levels of uric acid were measured in mice fed either the control diet or a HFCS-55 enriched diet for 30 weeks in the absence or presence of GW0742 (1 mg/kg/day). Data are means ± SD of three separate experiments for Western blot analysis and means ± SD of six animals/group for serum uric acid measurement. ★ $P < 0.01$ versus Control.

Figure 5. Development of albuminuria in animal chronically treated with HFCS-55 and its reversal by GW0742 administration. Urinary albumin:creatinine ratio (ACR) was measured in mice fed either the control diet or a HFCS-55 enriched diet for 30 weeks in the absence or presence of GW0742 (1 mg/kg/day). Urine were collected and ACR was measured16 weeks after starting the drug treatment. Data are means ± SD of six animals/group. ★ $p < 0.01$ versus Control.

Figure 6. GW0742 prevents HFCS-55-induced levels of neutrophil infiltration markers in the mouse kidney. Myeloperoxidase (MPO) activity (Panel A) was measured by spectrophotometric analysis and ICAM-1 (Panel B) and iNOS (Panel C) protein expression was detected by Western blot analysis in mice fed on a standard (Control) or HFCS-55 diet in the absence or presence of GW0742 (1 mg/kg/day). Densitometric analysis of the bands is expressed as relative optical density (O.D.), corrected for the corresponding β-actin contents, and normalized using the related Control band. Data are means ± SD of three separate experiments for Western Blot and five animals/group for MPO. ★ $p < 0.05$ versus Control.

Figure 7. PPAR-δ upregulation induced by chronic GW0742 administration affects inhibits caspase-1 and IL-1β processing, which is dependent on NLRP3, in the mouse kidney. Alterations in renal expression of PPAR-δ, NLRP3, procaspase-1, activated caspase-1, pro-IL-1β and cleaved IL-1β were measured by Western blot analysis (Panel A) in liver homogenates of mice fed on a standard (Control) or HFCS-55 diet in the absence or presence of GW0742 (1 mg/kg/day). Serum levels of IL-1β were analyzed by enzyme-linked immunosorbent assay (ELISA) (Panel B). Densitometric analysis of the bands is expressed as relative optical density (O.D.), corrected for the corresponding β-actin contents, and normalized using the related Control band. Data are means ± S.D. of three separate experiments for Western Blot and five animals/group for ELISA. ★ $p < 0.01$ versus Control.

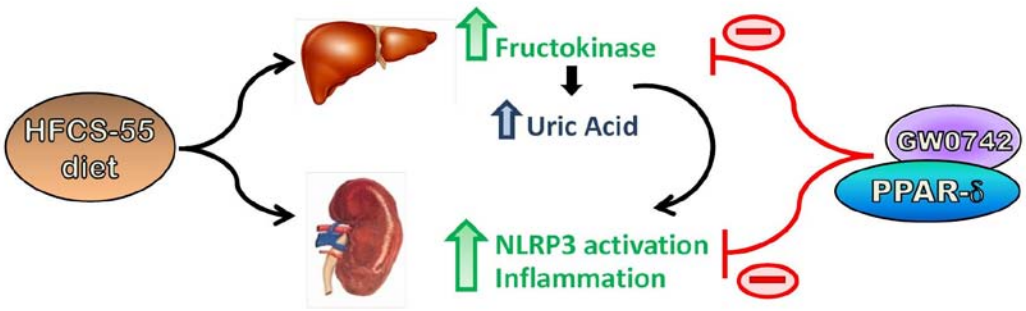
HFCS-55
diet
Fructokinase
Uric Acid
NLRP3 activation
Inflammation
GW0742
PPAR-δ

Figure 1

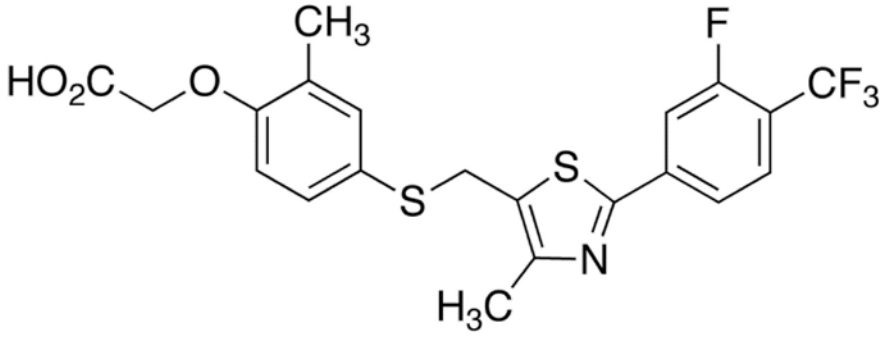

GW0742

4-[[[2-[3-fluoro-4-(trifluoromethyl)phenyl]-4-methyl-5-thiazolyl]methyl]thio]-2-methylphenoxy] acetic acid

	EC_{50} (nM)
PPAR-δ	28
PPAR-α	8900
PPAR-γ	> 10000

Figure 2

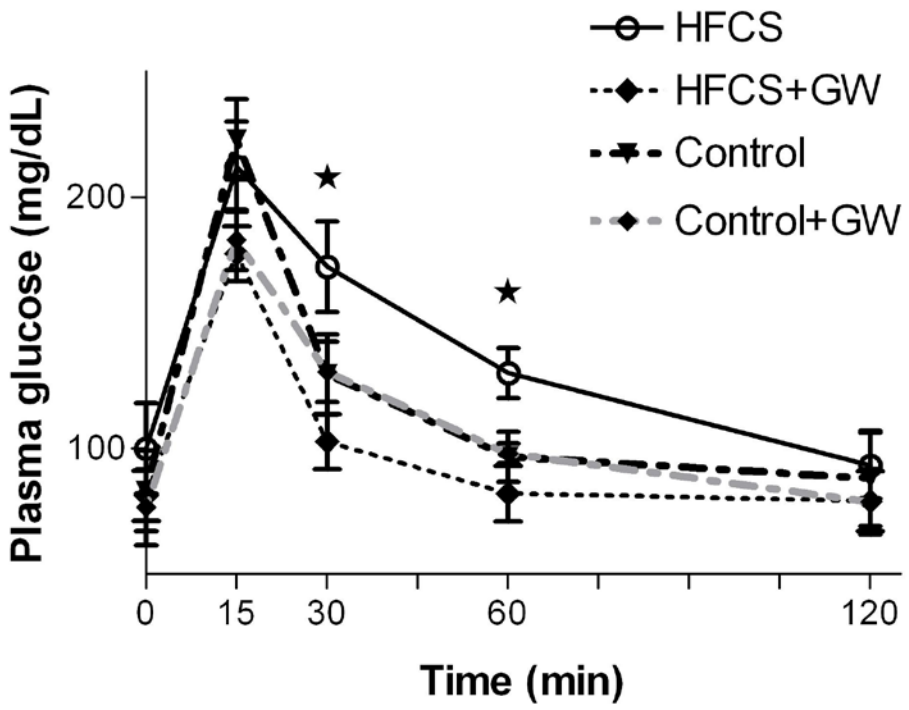
HFCS
HFCS+GW
Control
Control+GW
Plasma glucose (mg/dL)
200
100
0
15
30
60
120
Time (min)

Figure 3

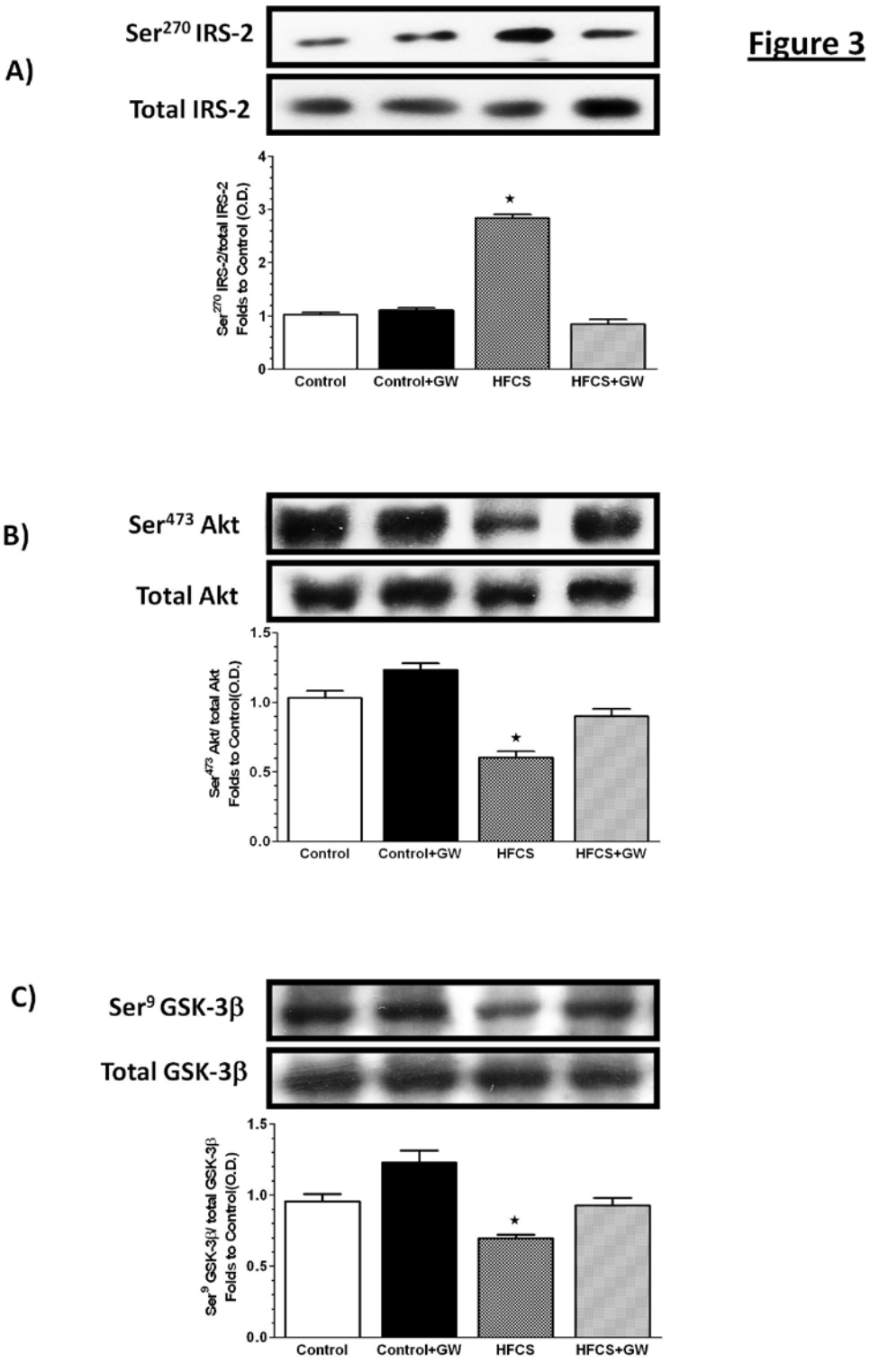
A)
Ser270 IRS-2
Total IRS-2
Ser270 IRS-2/total IRS-2 Folds to Control (O.D.)
Control
Control+GW
HFCS
HFCS+GW
B)
Ser473 Akt
Total Akt
Ser473 Akt/ total Akt Folds to Control(O.D.)
C)
Ser9 GSK-3β
Total GSK-3β
Ser9 GSK-3β/ total GSK-3β Folds to Control(O.D.)

Figure 4

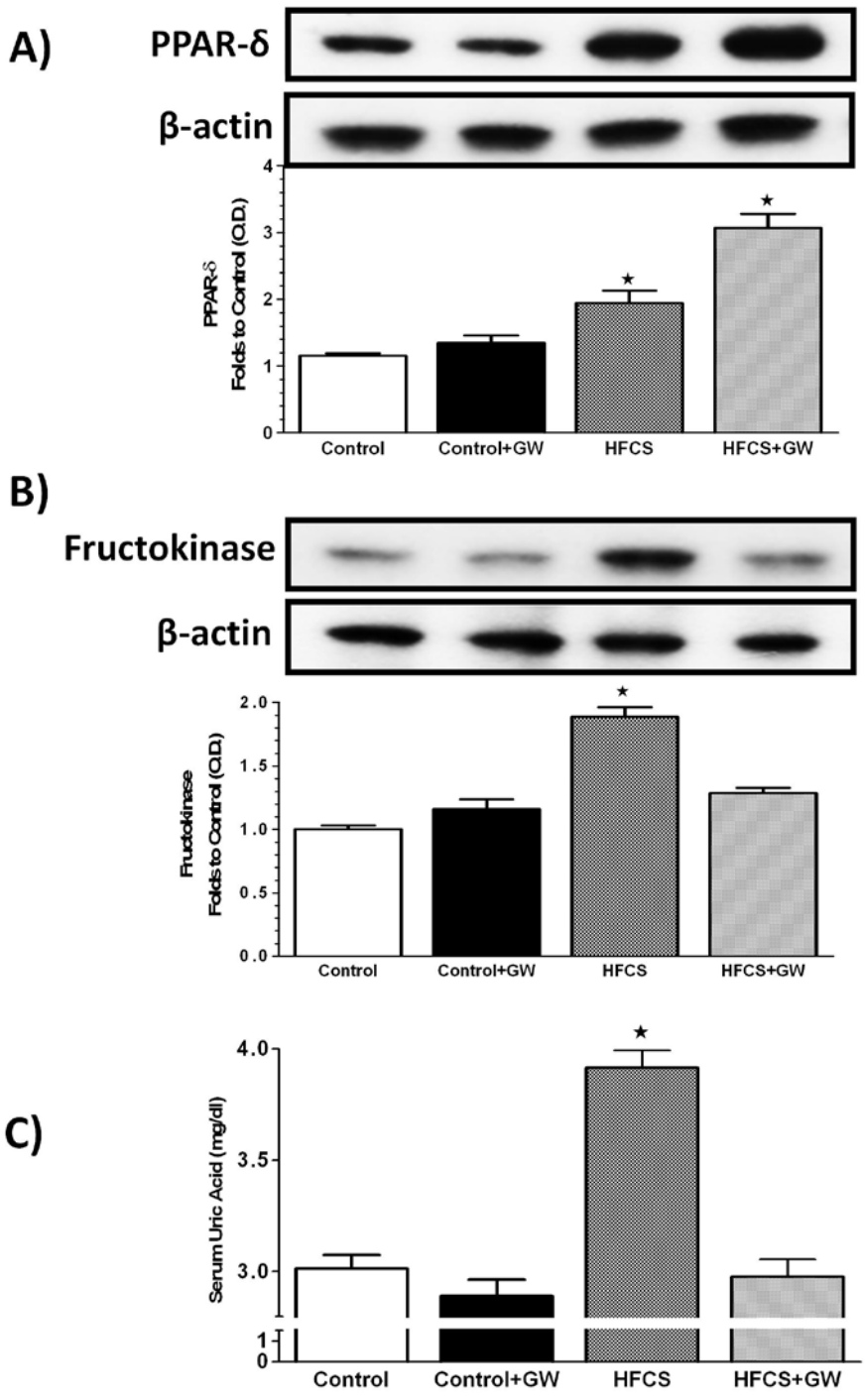
A)
PPAR-δ
β-actin
PPAR-δ Folds to Control (O.D.)
0
1
2
3
4
Control
Control+GW
HFCS
HFCS+GW
B)
Fructokinase
β-actin
Fructokinase Folds to Control (O.D.)
0.0
0.5
1.0
1.5
2.0
Control
Control+GW
HFCS
HFCS+GW
C)
Serum Uric Acid (mg/dl)
0
1
3.0
3.5
4.0
Control
Control+GW
HFCS
HFCS+GW

Figure 5

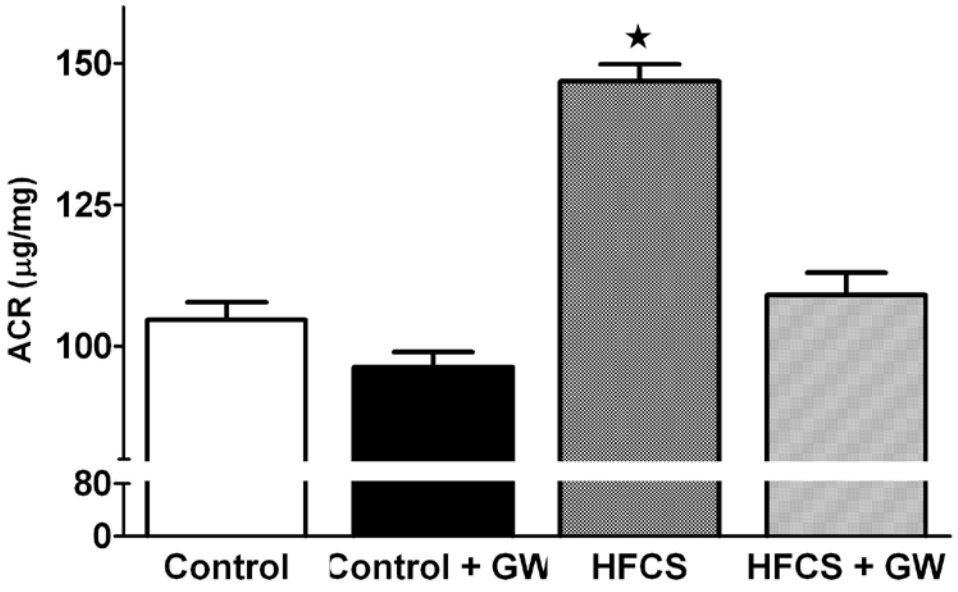

Figure 6

A)

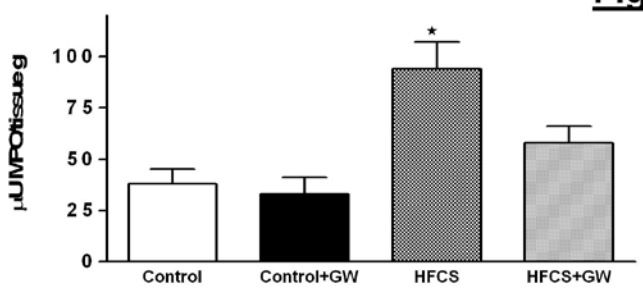
μUMPO/tissue g
100
75
50
25
0
Control
Control+GW
HFCS
HFCS+GW

B)

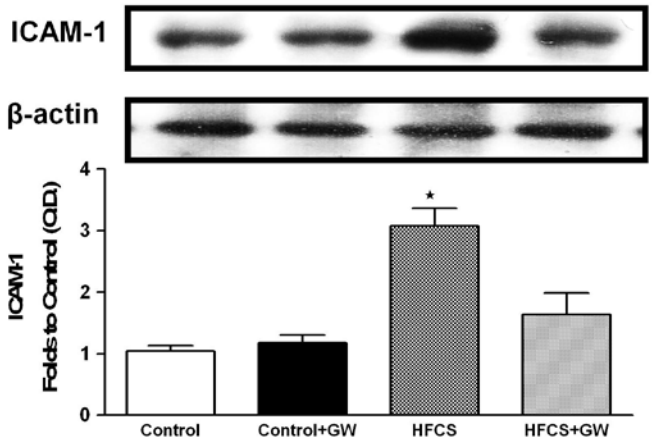
ICAM-1
β-actin
ICAM-1
Folds to Control (OD)
4
3
2
1
0
Control
Control+GW
HFCS
HFCS+GW

C)

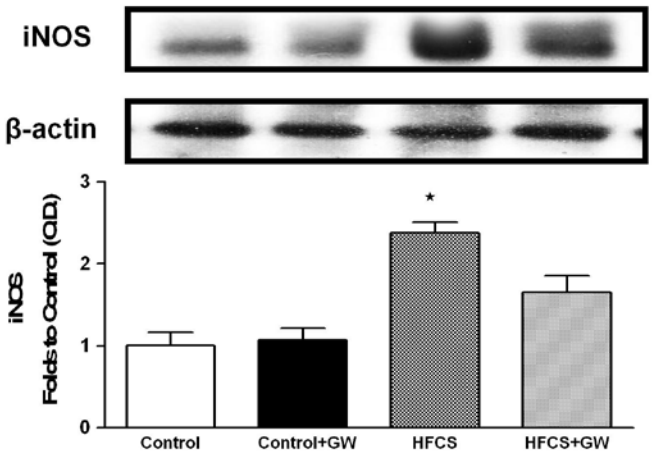
iNOS
β-actin
iNOS
Folds to Control (OD)
3
2
1
0
Control
Control+GW
HFCS
HFCS+GW

Figure 7

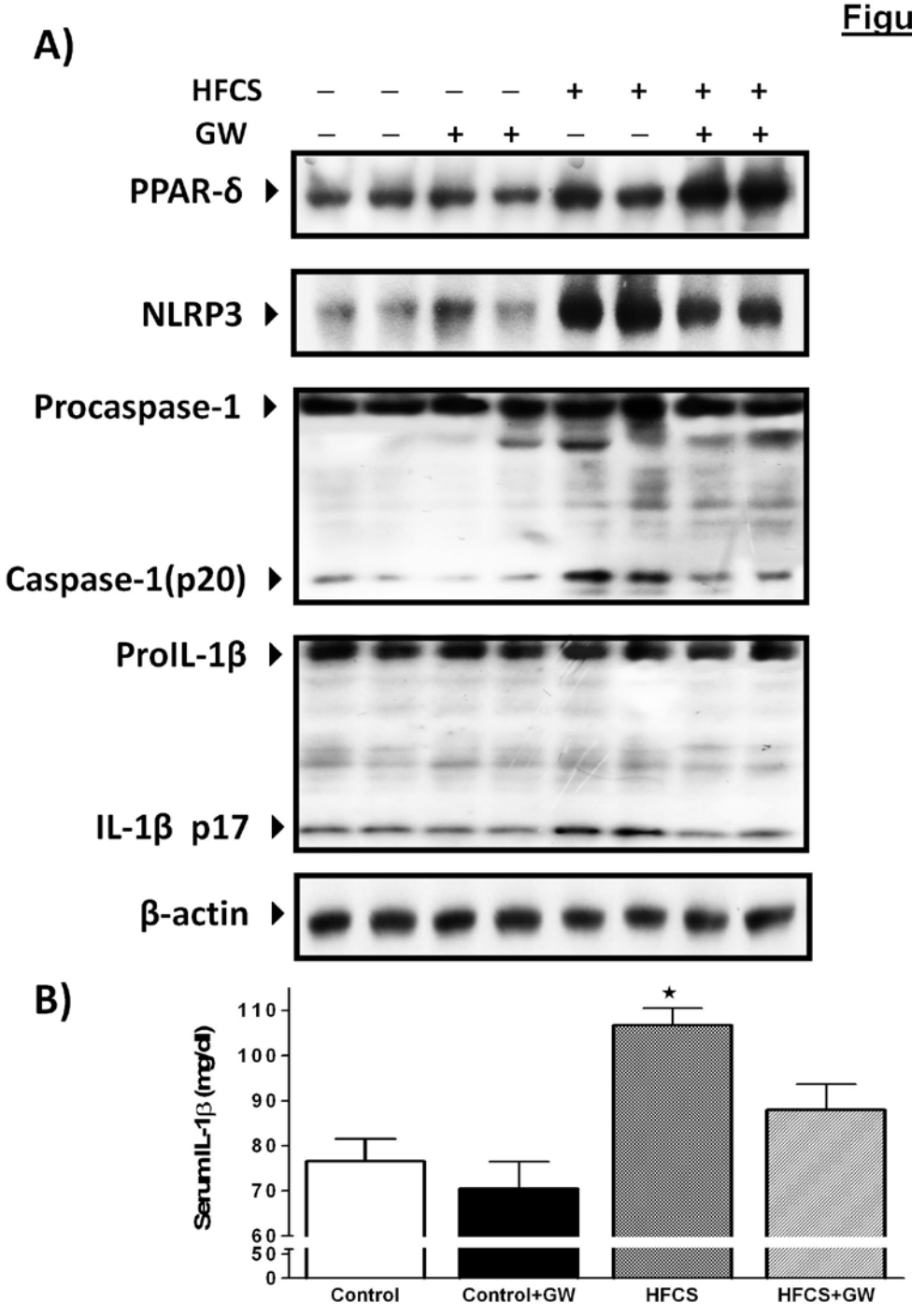
A)
HFCS – – – – + + + +
GW – – + + – – + +
PPAR-δ
NLRP3
Procaspase-1
Caspase-1(p20)
ProIL-1β
IL-1β p17
β-actin
B)
SerumIL-1β (mg/dl)
110
100
90
80
70
60
50
0
★
Control
Control+GW
HFCS
HFCS+GW